Surface-polarization electrooptic effect in a nematic liquid crystal

O. D. Lavrentovich, V. G. Nazarenko, V. M. Pergamenshchik, V. V. Sergan, and V. M. Sorokin

Institute of Physics, Academy of Sciences of the Ukrainian SSR, Kiev
(Submitted 31 August 1990; resubmitted 5 November 1990)
Zh. Eksp. Teor. Fiz. **99**, 777–802 (March 1991)

A new electrooptic effect was observed experimentally in a homeotropic layer of a nematic with a positive anisotropy of the permittivity and of the electrical conductivity. This effect appeared in an external vertical static electric field and was manifested by the appearance of circular or elongated domain structures due to static distortions of the director near the anode or cathode of a cell. The polarity of the effect depended on the nature of an orienting coating. The origin of the effect was the nematic surface polarization which was sufficiently strong ($\simeq 10^{-2}$ dyn$^{1/2}$) to induce an instability even under the conditions where other mechanisms (dielectric, flexoelectric, anisotropic electrohydrodynamic) impeded stability. Special attention was given to the separation of the surface polarization mechanism of the investigated effect from the flexoelectric and isotropic electrodynamic mechanisms. A hierarchy of static structures observed experimentally was clearly accounted for by a theory based on an equilibrium thermodynamic approach allowing for the anisotropic properties and for the real geometry of the system.

INTRODUCTION

An external electric field **E** applied to a nematic liquid crystal (NLC) can distort the director **n** and thus alter the optical properties of the nematic. The situations when the effect is due to dielectric, flexoelectric, or electrohydrodynamic mechanisms have been investigated quite thoroughly.[1] It has been suggested that the electrooptic effects may appear also because of the surface polarization of an NLC which results from breakdown of the degeneracy condition $\mathbf{n} \equiv -\mathbf{n}$, applicable to the director at a boundary (interface), and which is due to the polar nature of the interaction between the NLC molecules and the ambient medium or due to a change in the scalar part of the order parameter of the NLC. This possibility was first pointed out in Ref. 2 and then in Ref. 3.

Some experiments have revealed features of the behavior of NLCs which could be due to the surface polarization (see, for example, the review in Ref. 4). However, it is difficult to separate unambiguously the contribution of such polarization. In particular, the effects observed as a result of periodic compression of an NLC layer[5,6] could be due to flow of matter and certain special features, manifested in the electroreflection experiments[7] or in second harmonic generation in a surface layer of an NLC,[8] could represent the contribution of the ionic component.[4] These secondary phenomena were suppressed in another investigation,[9] but it was not possible there to separate clearly the surface polarization mechanism from the flexoelectric contribution. The problem of identifying the surface polarization in the electrooptic effects and determination of its parameters is therefore still topical. The present paper reports an attempt to solve this problem both experimentally and theoretically.

In the experimental part (Secs. 1–4), after formulation of the problem (Sec. 1) and description of the method (Sec. 2), we shall report the results of investigations designed to separate the surface-polarization electrooptic effect from the background of the other contributions, particularly the electrodynamic (Sec. 3) and flexoelectric (Sec. 4). The theoretical part of the paper gives a general formulation of the problem of deformations induced by an electric field in an NLC layer exhibiting surface polarization (Sec. 5) and this is followed by a systematic discussion of phase transitions to states with different geometries (Appendices I–III). The hierarchy of the states due to the interaction of the surface polarization with an electric field is discussed in Sec. 6.

EXPERIMENTS

1. Formulation of the problem

The problem in the experiments was the selection of the cell geometry which would ensure, firstly, the highest possible values of the polarization P_s, secondly, would make it easy to determine the polarization-induced tilt of the director **n** by optical methods and, thirdly, would make it possible to separate the polarization mechanism of the tilt from the dielectric, electrohydrodynamic, or flexoelectric mechanisms. All these conditions are satisfied by a cell with a homeotropically oriented NLC, which is characterized by a positive anisotropy of the permittivity ($\Delta\varepsilon > 0$) and of the electrical conductivity ($\Delta\sigma > 0$). The external electric field is assumed to be vertical, i.e., $\mathbf{E} \| \mathbf{n}$. This geometry eliminates the Fréedericksz or Carr–Helfrich effects,[1] i.e., it avoids a reorientation of **n** because of the dielectric or anisotropic electrodynamic torques. Moreover, in the initial state the cell observed under a polarizing microscope is totally dark, since the optic axis of the NLC coincides with the microscope axis; this makes it possible to detect readily the changes in the orientation of **n** because textures then become visible.

The selected experimental geometry does not, however, allow us to eliminate *a priori* two secondary effects: flexoelectric and isotropic electrohydrodynamic. In view of the important role of these effects in the interpretation of our results, it is essential to consider in greater detail the published data on this topic.

As pointed out, when the conditions $\Delta\varepsilon > 0$ and $\Delta\sigma > 0$ are satisfied, neither the dielectric nor the anisotropic electrohydrodynamic instabilities can appear in a homeotropic NLC layer. In spite of this, rounded or striped domain structures have been observed[9–11] on application of a static vertical field. This effect has a threshold: domains appear only

 0038-5646/91/030431-14$03.00

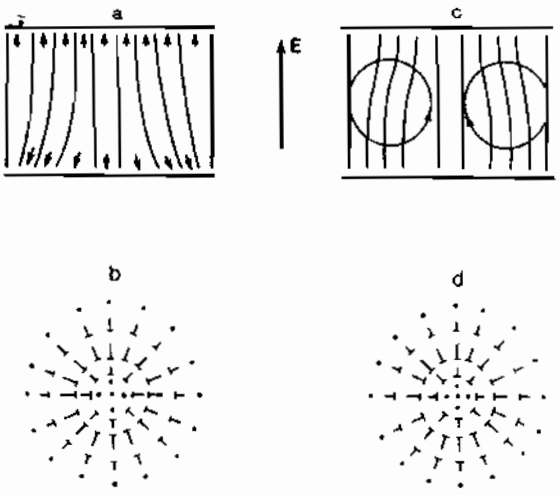

FIG. 1. Geometry of circular domains of the static (a, b) and dynamic (c, d) types in a homeotropically oriented layer of a nematic liquid crystal, induced by the surface polarization and the isotropic electrohydrodynamic mechanisms, respectively. Sections of domains by vertical (a, c) and horizontal (b, d) planes are shown. The arrows identify the directions of the surface polarization (a) and of the vortex flow in the liquid crystal (c).

when the field exceeds a critical value E_c. External manifestations of the instabilities reported in Refs. 9–11 are very similar (Fig. 1), but they have been interpreted invoking fundamentally different mechanisms.

For example, the tilt of a director from the initial vertical direction is explained in Refs. 10 and 11 by the isotropic electrohydrodynamic instability (Felici mechanism).[12] An argument used to support this explanation is the motion of foreign particles suspended in an NLC which travel between the center and periphery in circular domains,[10] and also a strong increase in the electrical conductivity under voltages exceeding the threshold, which is accounted for by the injection of charge carriers from the electrodes. The Felici mechanism resembles in many ways the convective motion of a liquid under the influence of a temperature gradient. In the present case this role is played by a gradient of the space charge density and, instead of the acceleration due to gravity, we have the electric field.[12] The isotropic electrohydrodynamic instability is a threshold effect[10–12] and appears only at values of E exceeding a critical field E_{c2}.

A fundamentally different interpretation of the instability of a homeotropically oriented NLC characterized by $\Delta\varepsilon > 0$ and $\Delta\sigma > 0$ is proposed in Ref. 9: it is based on the static nature of domain structures. A static field is found to tilt the director from the initial orientation and the effect is localized near the cell anode. It is postulated in Ref. 9 that this may be due to the flexoelectric effect and to the surface polarization of an NLC boundary, but the two mechanisms could not be separated.

As pointed out already, the external manifestations of the instabilities of both types are very similar. Moreover, the static[9] and dynamic[10–12] instabilities have electric-field thresholds. Therefore, the question of the true origin of the instabilities described in Refs. 9–12 requires an additional comparative analysis.

The above discussion allows us to formulate the experimental procedure for separation of the surface electrooptic effect in a homeotropic NLC film. The first stage is the separation of the instabilities due to the isotropic electrohydrodynamic mechanism from the static effect due to the flexoelectric and/or surface polarization mechanism. The differences should be manifested in at least three ways. Firstly, the domains due to the flexoelectric and/or surface polarization should not be accompanied, in contrast to the electrohydrodynamic domains, by vortex motion. Secondly, the static instability threshold E_{c1} need not be equal to the threshold E_{c2} of the isotropic electrohydrodynamic instability even if its effects appear in the same cell. Thirdly, the transition of an NLC to the isotropic liquid phase should suppress the former effect and not the latter (see, for example, Ref. 10).

During the second stage of the experiment, if it is found that domains can be of the static type, it is necessary to separate the two possible mechanisms—flexoelectric and surface polarization—of their appearance. Our plan for this separation involves the use of cells of two types, A and C, differing in respect of the nature of the orienting coatings and therefore in respect of the direction of the surface polarization vector $\mathbf{P}_s$ (with the homeotropic initial orientation retained in both cases). The polarization $\mathbf{P}_s$ can be reversed, as first pointed out in Ref. 13, by deposition on orienting coatings of surface-active substances such as lecithin whose molecules are amphiphatic.

2. Experimental methods

We investigated homeotropically oriented films of pentylcyanobiphenyl (5CB) which is a typical representative of compounds characterized by $\Delta\varepsilon > 0$ and $\Delta\sigma > 0$. The distribution of charges in the 5CB molecule $[C_5H_{11}(C_6H_4)_2CN]$ is such that the N atom is positively charged, whereas the C atom in the C≡N group is negative (see, for example, Ref. 14). This gives rise to a permanent dipole moment $\mu \approx 4.3$ D (Ref. 15), directed practically parallel to the long axis of the molecule and, consequently, perpendicular to the cell electrodes. An important feature of the 5CB molecule is its amphiphatic nature and capability of assuming different orientations on hydrophilic and hydrophobic surfaces. Following Ref. 13, we can expect the hydrophilic (polar) end of the molecule with the CN group to be oriented preferentially toward a hydrophilic coating (degreased surface) and the hydrophobic part of C_5H_{11} to tend to approach a hydrophobic coating, such as that created by a layer of a surface-active material on a hydrophilic substrate.

The cells consisted each of two pieces of glass with sputtered current-conducting films. We investigated cells with different coatings setting the homeotropic orientation of an NLC. In the classification of the cells we numbered the coating materials as follows:

In_2O_3:Sn	(200 Ω/□)	1
In_2O_3:Sn	(2×10^6 Ω/□)	1′
Silicone elastomer		2
SiO_2		3
Lecithin		4

In the cells which we denoted by the symbol $1 \equiv 1$ (the numbers represent the coating material and the identity sign represents schematically an NLC film), the homeotropic orientation was established by a pair of identical low-resistance In_2O_3:Sn electrodes. This material not only ensure the homeotropic orientation of 5CB, but was also stable in electric fields.

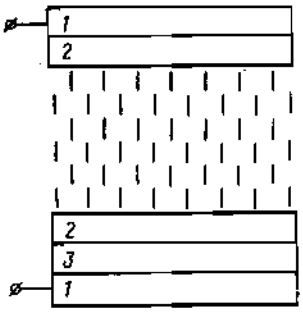

FIG. 2. Schematic representation of a measuring cell of the 12≡231 type.

Pairs of identical electrodes were selected also for symmetric cells of the 12≡21 type. The difference from the 1≡1 cells was this: both conducting surfaces were coated with a layer of a silicone elastomer ($(CH_3)_3SiO[(CH_3)_2SiO]_nSi(CH_3)_3$ where $n\sim2500$) of thickness amounting to several hundreds of nanometers. The additional orienting layer was assumed to alter the dipole polarization of the NLC at the surface and to change the conditions of carrier injection from the electrodes.[1]

A more effective prevention of carrier injection was ensured by cells of the 12≡231 type (Fig. 2) in which a layer of SiO_2, 120 nm thick, was deposited on one of the surfaces between In_2O_3:Sn and the silicone elastomer. The asymmetry of the 12≡231 cells made it possible to study also the polar nature of the resultant instabilities. Finally, we used also asymmetric cells of the 1≡1′ type in which one of the electrodes was a low-resistance In_2O_3:Sn layer and the other was a high-resistance In_2O_3:Sn layer (200 Ω/□ and 2×10^6 Ω/□, respectively). The use of these 1≡1, 12≡21, 12≡231, and 1≡1′ cells and a comparison of their parameters had the ultimate aim of separating the static and dynamic instabilities.

The second part of our task of separation of the surface polarization and flexoelectric contributions to static distortions was carried out by a comparative analysis of the 12≡21 cells with those of a new type: 124≡421. The silicone elastomer layer in the 12≡21 cells was hydrophilic and it set the preferential orientation of the CN polar groups in the 5CB molecules parallel to the substrate. The principal distinguishing feature of the 124≡421 cells was that the NLC was not in contact with the elastomer but with lecithin, whose molecules were diphylic, and became attached so that the polar part was in contact with the elastomer, thus establishing the opposite orientation of the 5CB molecules at the electrodes. The surface-active (surfactant) layer was formed by deposition of a 1% solution egg-yolk lecithin in ethanol on a layer of the elastomer. The substrates were dried for 3–4 h at 60 °C and only then was the cell filled with the NLC.

The electrical conductivity and permittivity of the investigated materials were as follows: in the case of 5CB these parameters were $\sigma_\parallel = 5\times10^{-8}\ \Omega^{-1}\cdot cm^{-1}$, $\sigma_\perp = 4.2\times10^{-8}\ \Omega^{-1}\cdot cm^{-1}$, $\varepsilon_\parallel = 18$, $\varepsilon_\perp = 4$; in the case of the silicone elastomer, the corresponding values were $\sigma_s = 6\times10^{-10}\ \Omega^{-1}\cdot cm^{-1}$ and $\varepsilon_s = 3.6$. These values will be used later in our theoretical analysis.

It should be stressed particularly that all these cells were not subjected to any rubbing operations in order to establish a preferential direction of the NLC. In other words, when the instabilities and tilts of the director from the vertical direction were observed, all the azimuthal orientations of the NLC molecules in the plane of the cell were equivalent. The only exception was a batch of the cells of the 12≡21 and 124≡421 types, which were rubbed in one direction when observations were made under a polarizing microscope.

This investigation was carried out on the nematic phase of 5CB and also on the isotropic liquid phase of this molecule. Temperatures were monitored to within 0.1 °C. A dc field was applied to a cell by a P4108 calibrated voltage source. The frequency characteristics were determined using a G6-16 oscillator. The polarization microscopic examination was carried out using a Peraval Interphako (Carl Zeiss, Jena) microscope modified with attachments for investigations in polarized light.

3. Static and dynamic instabilities

In this section we shall give the results of our investigation of domain instabilities in homeotropic NLC films placed inside the 1≡1, 12≡21, 12≡231, and 1≡1′ cells and subjected to vertical static or lf alternating electric fields. The experiments were carried out in order to determine the static and/or dynamic nature of the instabilities. The thickness of all the cells was the same: $D = 58\ \mu m$.

3.1. Polarizing microscope examination

3.1.1. Static field. The cell textures observed under the microscope depended on the applied field and one could identify arbitrarily three ranges of the field intensity E: in the range $0\leqslant E\leqslant E_{c1}$ the initial homeotropic orientation of the NLC was retained, whereas static domain instabilities were observed in the range $E_{c1}\leqslant E\leqslant E_{c2}$ and hydrodynamic motion of the NLC was observed when the field became $E\geqslant E_{c2}$. In the isotropic liquid phase there were no changes within the whole range $0\leqslant E\leqslant E_{c2}$; in fields $E\geqslant E_{c2}$ the motion of the isotropic liquid phase was exactly the same as in the nematic phase. The behavior in the various cells within these ranges of E will now be described in detail.

a) $0\leqslant E\leqslant E_{c1}$. In the initial state in the absence of the field a homeotropic texture was observed in all the cells. There was practically no transmission of light by the cell, because the director was oriented along the optic axis of the microscope. The homeotropic texture was retained also on application of a low voltage ($E\leqslant E_{c1}$). In this case the transmission of light could even decrease, which was clearly due to the further orientation of the NLC in the bulk caused by the dielectric mechanism (because 5CB was characterized by $\Delta\varepsilon>0$).

b) $E_{c1}\leqslant E\leqslant E_{c2}$. As the field was increased, it was found that cells began to transmit light from a certain threshold E_{c1}. The values of E_{c1} varied with the type of the cell (Table I) were within the range 1–4 V. The cause of such bleaching was the appearance, over the whole electrode area, of gray domains with vague outlines. Upon a further increase in the voltage to 6–7 V the domains assumed well-defined circular or slightly elongated forms (Fig. 3a) with four extinction branches. The homeotropic orientation was retained at the centers of the domains and in the gaps between them (when the sample was rotated in a horizontal plane these regions remained dark).

A detailed determination of the orientation of the direc-

TABLE I. Threshold fields corresponding to the appearance of static (E_{c1}) and hydrodynamic (E_{c2}) instabilities in cells of different types subjected to a static electric field.

Cell		E_{c1}, 10^5 V/m	E_{c2}, 10^5 V/m
anode	cathode		
1	1	0,6	1,0
1	1′	0,6	1,0
1′	1	>1,4	>1,4
12	21	0,12	1,2
12	231	0,8	1,7
132	21	0,8	2,1
124	421	0,16	>0,16
[9]		0,6	>0,6
[10]		–	1,6

Note. The measurements were carried out at 20 °C.

tor in the domains was carried out with the aid of a quartz wedge. Changes in the interference patterns on introduction of the wedge[16] between a sample and the microscope polarizer demonstrated that the distribution of the director in the horizontal plane was radially symmetric with the center of symmetry at the center of a domain (Figs. 1b and 1d). Moreover, the interference color of domains indicated that the maximum deviations of the director from the initial vertical position were localized at about three-quarters of the radius from the center. The phase delay $\delta = D(n' - n_o)$, was maximal in this region; here, $n' = n_e n_o (n_o^2 \sin^2\theta + n_e^2 \cos^2\theta)^{-1/2}$, n_e and n_o are the refractive indices of the extraordinary and ordinary rays, and θ is the angle of tilt of the director from the vertical.

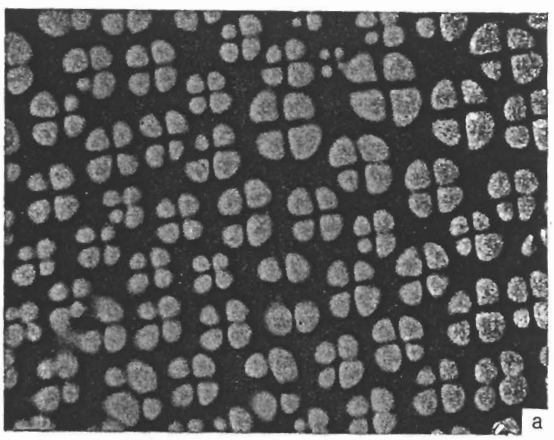

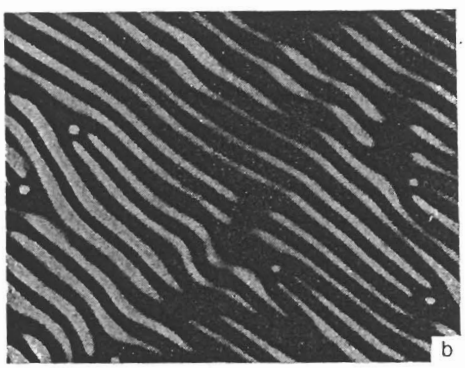

FIG. 3. Photomicrographs of textures of a homeotropically oriented layer of 5CB in cells of the $1 \equiv 1$ and $12 \equiv 21$ types subjected to a static electric field: a) unrubbed electrode surface; b) rubbed electrode surface.

It is interesting to note that refocusing of the microscope did not alter the positions of the bright and dark regions, in contrast to the electrohydrodynamic domains in the homeotropically oriented NLC films described in Ref. 10. Clearly, this difference was due to the different nature of the spatial localization of the domains: in the case of the electrohydrodynamic instability the maximum tilts of the director were observed in the interior of the cell, whereas in the present case we would expect the tilts to occur only in the surface layer.[9]

The polar nature of the effect and the localization of the distortions near one of the electrodes were manifested also in the following ways. One of the silicone elastomer surfaces in a cell of the $12 \equiv 21$ type was rubbed over the whole of its area along one direction. The second surface remained unrubbed. When the electrode with the rubbed orienting coating was used as the anode, the domains were no longer circular but strongly elongated with the stripe shape (Fig. 3b) and the director was reoriented perpendicular to the direction of rubbing. When the polarity was reversed (so that the unrubbed surface served as the anode), the domains were once again circular, as in the case of completely symmetric cells with unrubbed surfaces. These observations confirmed the hypothesis that the domain instability effect was of polar nature and was due to tilts of the director near one of the surfaces of the cell (in the presence of the silicone elastomer coating this occurred at the anode, in agreement with the results reported in Ref. 9).

The polar nature of the domain instabilities observed in fields $E_{c1} \leqslant E \leqslant E_{c2}$ was manifested clearly in the experiments carried out using cells of the $1 \equiv 1'$ type. The domains appeared when the low-resistance electrode was used as the anode. The bleaching threshold E_{c1} was 0.6×10^5 V/m, i.e., it agreed with the value of E_{c1} obtained for the symmetric $1 \equiv 1$ cells (Table I). When the polarity of the field was reversed, the instability did not appear even for $E \approx 1.4 \times 10^5$ V/m, which could have been due to the weak polarizability of the high-resistance electrode because of the characteristic features of its structure.

The results of our investigation of cells of the $12 \equiv 231$ type were particularly interesting. We expected the asymmetry of these cells to influence electrohydrodynamic processes but not the static instability. We did indeed find that in fields $E_{c1} \leqslant E \leqslant E_{c2}$ there were circular static domains in these cells and the threshold of appearance of these domains ($E_{c1} = 0.8 \times 10^5$ V/m) was independent of the field direc-

tion (Table I). These observations agreed well with the hypothesis of the surface-polarization and/or flexoelectric mechanism of the instability in the range $E_{c1} < E < E_{c2}$. In fact, since the NLC layer on both surfaces was in contact with identical silicone coatings, the presence of the SiO_2 layer under one of them (Fig. 2) could not have had a significant influence on the formation and parameters of the surface polarization layer of the NLC, and it should have had even less influence on the flexoelectric coefficient of the nematic. Consequently, this layer should not alter the instability threshold E_{c1}. The SiO_2 layer could block partly the carrier injection from the electrode in question and prevent the development of the electrohydrodynamic instability, at least for one of two possible field directions. These quantitative ideas were confirmed by our experimental data: it is clear from Table I that the value of E_{c1} was the same for both polarities and that E_2 depended strongly on the polarity.

The most important result of our polarizing-microscope examination was the static nature of the distortions of the director in the domains in fields below E_{c2}. The absence of the motion of matter in the nematic and isotropic phases was checked by two methods. In the first we used small (0.5–5 μm) impurity particles. In the range $0 < E < E_{c2}$ (corresponding to a voltage of 6–7 V) they remained immobile. In the second method we introduced a dye (methyl red) from one end of the cell and observed under the microscope the motion of its diffusion front penetrating the pure part of the NLC. The velocity of such motion was not affected by the field or by the appearance of the domains, although we would expect the velocity to increase in the presence of the electrohydrodynamic instability.[17]

c) $E > E_{c2}$. The static nature of the domains was disturbed by voltages in excess of 6–7 V. Under the microscope we were able to detect the motion of tiny particles dragged by the flow of the NLC. The external shape of the domains changed only slightly. One should mention that the brightness of the domains decreased in this range of fields. Moreover, refocusing of the microscope resulted in transposition of the dark and bright regions, similar to the observations reported in Ref. 10 for the electrohydrodynamic domains. In the isotropic liquid phase we detected the flow of matter which appeared in fields $E > E_{c2}$ in cells of all the types.

The results led us to the conclusion that the homeotropic layer of the NLC with $\Delta\varepsilon > 0$ exhibited two types of the threshold instability in a vertical static field: a static instability due to the surface polarization and/or the flexoelectric effect, and also the isotropic electrohydrodynamic instability. It seemed appropriate to compare therefore the threshold values E_{c1} and E_{c2} (Table I) for different types of cell and to relate them to the instability mechanisms.

We shall begin by pointing out the differences between manifestations of the effects in the NLC and isotropic liquid phases. In the NLC we could distinguish two instability thresholds, E_{c1} and E_{c2}, whereas only one threshold, associated with the motion of matter and coinciding with E_{c2}, was observed for the isotropic liquid phase. This observation supported additionally the postulated mechanism of the isotropic electrohydrodynamic instability of the NLC in the range $E > E_{c2}$, because it should not depend significantly on the nature of ordering of the liquid.[10,12] We shall now discuss the relationship between E_{c1} and E_{c2} for the NLC phase. It is clear from Table I that the deposition of an additional silicone elastomer coating or of an SiO_2 film on the electrodes increased the electrohydrodynamic instability threshold E_{c2}. This increase in E_{c2} agreed with the hypothesis that the dielectric (insulating) layers prevented the injection of carriers from the electrodes. On the other hand, this silicone coating reduced considerably the static instability threshold E_{c1}. This could be explained in a natural manner using the surface polarization mechanism of the instability in the range $E_{c1} < E < E_{c2}$: in view of the hydrophilic nature of the silicone elastomer, we could expect it to orient more effectively the polar CN groups of the 5CB molecules at the interface with the nematic than at the untreated electrode surface.

Finally, it was interesting to compare our results with those of Refs. 9 and 10. We included in Table I appearance thresholds of the static[9] and electrohydrodynamic[10] instabilities determined for cells with indium oxide electrodes covered by a surfactant layer. The investigation reported in Ref. 10 was concerned with 5CB, whereas that described in Ref. 9 dealt with its analog 7CB ($\Delta\varepsilon \approx 10$). Clearly, the results of Ref. 9 were close to our values of the E_{c1} threshold for static deformations, whereas the values given in Ref. 10 were close to the E_{c2} threshold of the electrohydrodynamic instabilities.

3.1.2. Low-frequency alternating field. The application of an lf alternating field to homeotropically oriented NLC layers also gave rise to domain instabilities. Unfortunately, it was not possible to separate the domains with the static distribution of the director from the dynamic distribution and thus identify the two thresholds E_{c1} and E_{c2}, because a change in the polarity resulted in fluctuations of the domains at the frequency of the field even in the range $E_{c1} < E < E_{c2}$. Such fluctuations were due to alternate appearance of the instability at the electrodes. Therefore, we determined only one threshold voltage U_c corresponding to the onset of bleaching of the cell. The nature of the domains should affect above all the nature of the frequency dependences of U_c. The results of a determination of the latter are presented in Fig. 4.

The optical characteristics of the $1 \equiv 1$ cells are very specific and are determined by both the intensity and the frequency of the applied field. At low frequencies ($f < 0.1$ Hz) the threshold voltages were low (close to the values of $E_{c1}D$) and the domain textures were identical with those

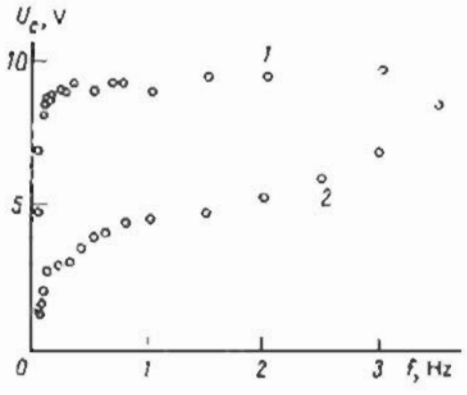

FIG. 4. Dependences of the threshold voltages on the frequency of the applied field: 1) cell of the $1 \equiv 1$ type; 2) cell of the $12 \equiv 21$ type.

observed in static fields of intensity $E_{c1} < E < E_{c2}$ (apart from fluctuations of the domains at the field frequency). An increase in the frequency increased strongly the threshold. At voltages corresponding to $E_{c2}D$ the domain structure changed slowly: the domains became elongated, the brightness decreased, and the dimension of the bleached regions became greater. Refocusing of the microscope resulted in transposition of the bright and dark regions, typical of the electrohydrodynamic domains.

It was worth noting the fact that in the range $f > 0.1$ Hz the threshold voltage was practically independent of the frequency. This was in agreement with the postulate of the isotropic electrohydrodynamic mechanism in the range $f > 0.1$ Hz when the voltage was $U_c \approx E_{c2}D$, because the absence of the dependence of U_c on f was a typical feature of the Felici mechanism at low frequencies.[1] In the range of $f < 0.1$ Hz, where the bleaching threshold was less and corresponded approximately to $E_{c1}D$, the rise in U_c on increase in f agreed with the model of static polar deformations proposed in Ref. 9 (according to estimates obtained in Ref. 9, we should have $U_c \propto f^{1/2}$). Therefore, cells of the $1 \equiv 1$ type could obviously be used to observe both types of instability: the static at frequencies $f < 0.1$ Hz with a threshold $U_c \approx E_{c1}D$ and also the electrohydrodynamic instabilities at frequencies $f > 0.1$ Hz with a threshold $U_c \approx E_{c2}D$. To avoid ambiguity, it should be stressed that the electrohydrodynamic motion obviously appeared also in strong fields at frequencies $f < 0.1$ Hz, but for the reasons given above it was not possible to identify such motion and to distinguish a threshold other than E_{c1}. Conversely, the static instability could form also in the range $f > 0.1$ Hz, by the threshold of its appearance in this range because of the dependence $U_c > f^{1/2}$ was probably higher than the electrohydrodynamic instability threshold.

In cells of the $12 \equiv 21$ type with a silicone coating the nature of the domains in the frequency range up to 3 Hz did not differ in any way from the domains that appeared in a static field. The frequency dependence of the threshold voltage U_c was parabolic: $U_c \propto f^{1/2}$, in agreement with the static instability mechanism. The rise of U_c with the frequency obtained for the $12 \equiv 21$ cell was smoother than that for the $1 \equiv 1$ case. This was not in conflict with the polarization or the flexoelectric mechanisms: a theoretical analysis given in Ref. 9 demonstrated that the rate of change of U_c with the frequency depended on the surface polarization and on the anchoring energy. These parameters were clearly different for the $1 \equiv 1$ and $12 \equiv 21$ cells.

3.2. Current-voltage characteristics in static fields

It is known that cells containing an NLC and subjected to a static electric field may exhibit carrier injection at the interface between the liquid crystal and the electrodes.[9-11] The existence of such injection has been demonstrated also for homeotropically oriented nematic films characterized by $\Delta\varepsilon > 0$ using the current-voltage characteristics.[10,11] It was pointed out there that the appearance of domain instabilities was accompanied by a steep rise of the electrical conductivity of the cells. Moreover, the change in the density of the current J flowing through the cell due to a change in temperature T obeyed the Richardson expression for the thermionic emission current:

$$J = AT^2 \exp(-F/kT), \qquad (1)$$

where k is the Boltzmann constant, and A and F are constants depending on the nature of the electrodes, their treatment, and the applied field.

The current-voltage characteristics of our cells (Fig. 5) differed qualitatively from those reported in Refs. 10 and 11. Firstly, at voltages corresponding to the threshold E_{c1} of the domain motion there was no significant increase in the current across the cell. This was manifested particularly clearly in cells of the $1 \equiv 1$ type whose current-voltage characteristics were practically linear between zero and 8 V, in spite of the fact that static domains appeared already at 3.5 V. Secondly, the change in the current density of temperature did not obey the thermionic emission law and, at least in the range $E_{c1} < E < E_{c2}$, the experimental dependences plotted using the coordinates $\log(J/T^2)$ and $10^3/T$ could not be described by a linear dependence, contrary to the predictions that follow from the Richardson law (1) (see Fig. 6). Moreover, it is clear from Fig. 6 that the temperature dependences of the current were described satisfactorily by the usual exponential expression

$$J = J_0 \exp(-U/kT),$$

corresponding to the activated mechanism of electrical conduction. We should mention also that the domain appearance threshold E_{c1} was practically independent of the current through a cell, as demonstrated by the current-voltage characteristics of the $12 \equiv 231$ cell (Fig. 5c). The current through the cell depended strongly on the polarity of the applied field (Fig. 5c), which was due to the fact that one of the cell electrodes was coated by a layer of SiO_2 preventing carrier injection. On the other hand, the domain appearance threshold E_{c1} was unaffected by neither polarity reversal nor by variations of temperature. These observations were also in agreement with the surface mechanism of the instability observed in the range $E_{c1} < E < E_{c2}$.

We shall now summarize all that was said in Sec. 3. The domain structures in homeotropically oriented NLC films of 5CB characterized by $\Delta\varepsilon > 0$ and $\Delta\sigma > 0$, which were characterized in a vertical static field or in an lf alternating electric field, by two values of the instability threshold: E_{c1} and E_{c2}. In the range $E_{c1} < E < E_{c2}$ we found that static domains appeared in the NLC and that in the range $E > E_{c2}$ the domains were associated with the vortex motion of matter. Textures of both types of domain were indistinguishable; we could simply point out that in the case of the electrohydrodynamic domains when the microscope was refocused the dark and bright parts of the texture became transposed, whereas the static domains showed no such effect. In the isotropic liquid phase the instability appeared only in the fields $E > E_{c2}$ and was associated with the flow of matter. The values of E_{c1} and E_{c2} depended strongly on the nature of the orienting coatings in the cell and it was found that the polar coatings (such as the silicone elastomer used in the present study) tended to reduce strongly the value of E_{c1}, whereas the coatings preventing carrier injection (SiO_2 layers) increased E_{c2}. The appearance of the domain instabilities in $E = E_{c1}$ was unrelated to carrier injection, as deduced from the current-voltage characteristics and the temperature dependences of the current. In lf alternating fields the appearance threshold of the static domains increased with the field frequency (proportionally to $f^{1/2}$). The results summarized above lead to

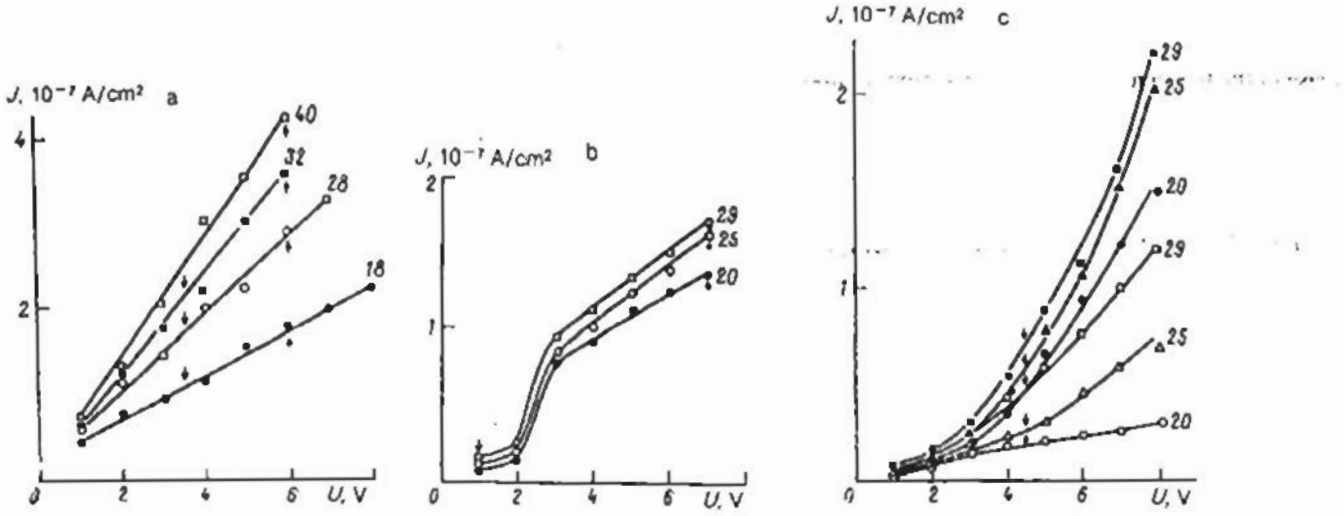

FIG. 5. Current-voltage characteristics obtained at different temperatures (the numbers alongside the curves give T in degrees Celsius) in cells of the 1≡1 (a), 12≡21 (b), and (c) 12≡231 types. The symbols ●, ▲, and ■ apply in this situation when the anode is the 132 coating; the symbols ○, △, and □ correspond to the 21 coating. The arrows identify the threshold voltages as follows: ↓ represents E_{c1} (U_{c1}), and ↑ corresponds to E_{c2} (U_{c2}).

the conclusion that the domain structures observed in fields $E_{c1} < E < E_{c2}$ are due to the surface polarization and/or the flexoelectric instability of the NLC, whereas those observed in the range $E > E_{c2}$ are due to the isotropic electrohydrodynamic instability. In the next section we will report an investigation of the static effect based on a comparative analysis of the results obtained in cells of the 12≡21 and 124≡421 types.

4. Surface polarization and flexoelectric effect associated with the formation of static instabilities

We investigated cells of the 12≡21 and 124≡421 types with the gap $D = 10$–100 μm thick in fields of intensities $0 < E < E_{c2}$, i.e., we investigated only the static instabilities.[1] The textures in the 124≡421 and 12≡21 cells observed in this range of E were similar to those obtained as a result of static deformation and described in Sec. 3 above. However, the electrooptic response of the 124≡421 and 12≡21 cells differed in one fundamental respect. Refocusing of the microscope, reversal of the field polarity, and shift of the glass plates in the cells relative to one another demonstrated that the distortions of the director which resulted in bleaching of the textures were localized in the 12≡21 cells near the anode and in the 124≡421 cells near the cathode. Therefore, we labeled the 12≡21 cells type A and the 124≡421 cells type C. This polar nature of the effects was manifested also in the behavior of the cells when one of the surfaces was rubbed. Elongated domains appeared only when the rubbed surface served as the anode in the A cells and as the cathode in the C cells.

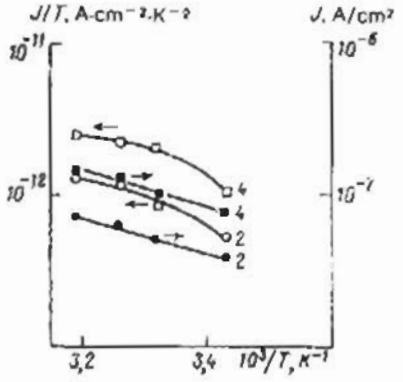

FIG. 6. Temperature dependence of the current in a cell of the 1≡1 type obtained at different voltages. The numbers alongside the curves the voltages in volts.

The fact that the distortions of the director were localized near the anode in the A cells and near the cathode in the C cells played a key role in the understanding of the nature of the effect. The phenomena in the A cells in the range $E_{c1} < E < E_{c2}$ were analogous to those described in Ref. 9 and could be explained qualitatively (but not quantitatively) by the flexoelectric effect, whereas the C-type instability had not been described before and could not be due to the flexoelectric effect.

We shall consider this question in greater detail. The flexopolarization of an NLC governed by the nature of the distortions of the director is[1]

$$\mathbf{P}_f = e_1 \mathbf{n}\,\mathrm{div}\,\mathbf{n} + e_3[(\mathrm{rot}\,\mathbf{n})\mathbf{n}], \qquad (2)$$

where e_1 and e_3 are the flexocoefficients, and it makes a contribution amounting to $-(\mathbf{P}_f\mathbf{E})$ to the free energy density. If the field E is directed vertically and the coefficients obey $e_1 + e_3 = e > 0$, which is true of 5CB (Ref. 19), the energy of the system decreases because of the tilts of n near the cathode (Fig. 7). This can be used to explain quantitatively the effect in an A cell except for the fact that the flexoinstability requires the suppression of the dielectric moment which stabilizes the homeotropic orientation of n and ensures that the following condition is obeyed (Ref. 9):

$$e^2 > \frac{1}{4\pi}\Delta\varepsilon K_3,$$

where K_3 is an elastic constant. In the case of 5CB this condition is known to be disobeyed, because $e = 1.5 \times 10^{-4}$ dyn$^{1/2}$ (Ref. 19), $\Delta\varepsilon \approx 14.2$, and $K_3 = 9.8 \times 10^{-7}$ dyn (Ref. 20). As far as the C instability is concerned, the flexopolarization in the $e > 0$ case can only hinder the appearance of the instability (as demonstrated in Fig. 7), because the induced flexoelectric moment caused by deformation of the director near

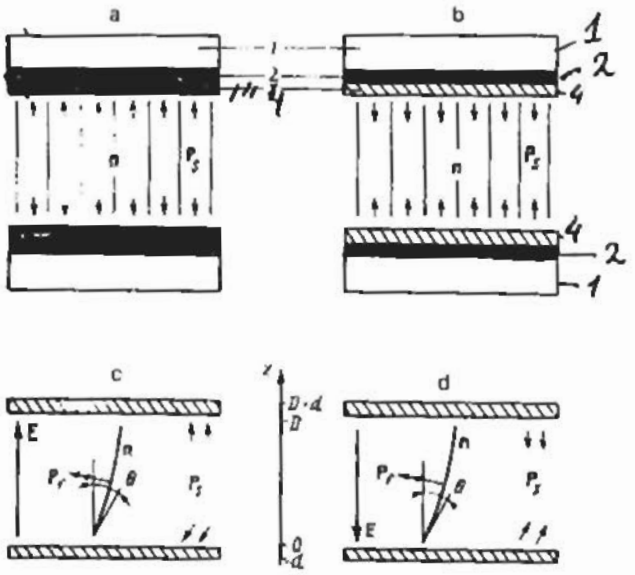

FIG. 7. Measuring cells in the geometry of instabilities in a homeotropic layer of 5CB in an external vertical field E: a), b) initial reorientations; the arrows show the nominal orientations of the dipole moments of the 5CB molecules at the surfaces of cells of the A type (a) and of the C type (b). The tilts of the director n in the external field are shown schematically near the anode in an A cell (c) near the cathode is a C cell (d). The thickness of the 5CB layer is D, and the thickness of the orienting coating on the electrodes is d. A silicone elastomer is used in the A cells and an elastomer with an additional layer of lecithin is used in C cells.

the cathode is opposite to E. In other words, the static deformation in the C cells cannot be due to the flexoelectric mechanism.

The experimental data can be explained if we allow for the surface polarization $\mathbf{P}_s$ of the NLC making a contribution $-(\mathbf{P}_s\mathbf{E})$ to the free energy, similar to the flexoelectric contribution. Since the use of an inverting layer of lecithin in the samples, the polarizations $\mathbf{P}_s$ in the A and C cells are different (Figs. 7a and 7b), it follows that if $|P_s|$ is sufficiently high, we can expect an anode instability in the A cells and a cathode instability in the C cells (Figs. 7c and 7d). In the C cells the destabilizing moment can only be due to the surface polarization; the flexoelectric and dielectric moments play a stabilizing role.

It follows from all this discussion that the main task of the experimental part of our study was fulfilled: it was found that the application of an electric field to a homeotropically oriented NLC film with $\Delta\varepsilon > 0$ and $\Delta\sigma > 0$ can cause tilts of the director which are due to the surface polarization of the NLC and are unrelated to the flexoelectric or electrohydrodynamic mechanisms.

The main physical reason for the appearance of the surface polarization in this situation should therefore be the difference between the interactions of the different ends of the 5CB molecules with the substrates. Firstly, this provides a natural explanation of the change in the polarity of the distortions of the director in the A and C cells and, secondly, the 5CB molecule is itself amphiphatic and contains the polar CN group at one end and the hydrophobic C_5H_{11} chain at the other.

The main physical reason for the surface polarization of the NLC may be a mechanism associated with gradients of the modulus of the order parameter ∇S. Even when the chemical interactions of the ends of the molecules with the surface are the same, there may be a change in the degree of ordering S at the interface and this may give rise to a macroscopic polarization $\mathbf{P}_s \propto \nabla S$ (known as the ordering electricity).[21] There are grounds for assuming however that this mechanism does not predominate in the experiments described above. Firstly, this instability was observed by us at temperatures quite far from the transition from the NLC to the isotropic liquid state; therefore, large values of ∇S would be unlikely. Secondly, our experiments failed to reveal any significant changes in E_{c1} as a result of heating of a sample. Thirdly, it was unlikely that the deposition of a lecithin layer on the elastomer surface could alter not only the value of ∇S, but also its direction; the change in the direction would be necessary to account for the differences in the behavior of the A and C cells. Finally, the experimentally determined[22] bias of the material constants associated with the "ordering polarization" were found to be relatively small, of the order of the flexocoefficients e, i.e., they were insufficient to initiate an instability.

The physical picture of the instability described above would be incomplete without a theory accounting for the appearance of static domain structures as a result of the interaction between an applied electric field and the surface polarization. Such a theory will be developed in the next sections of this paper.

THEORY

6. Formulation of the problem and general relationships

Our experiments thus demonstrate that when the external field is increased to E_{c1}, the homeotropic state of our NLC layer becomes unstable and it assumes a domain state in which there is no macroscopic motion of the liquid crystal. Consequently, it should be possible to explain this effect in the framework of equilibrium thermodynamics. If this approach is adopted to a situation in which a current flows through a sample, the effects of the anisotropy of the permittivity and of the conductivity of the nematic become of prime importance. An allowance for these effects gives rise to difficulties related to the need to minimize nonlocal functionals,[23] which in our case are complicated by the need to deal with three-domain structures and not with one-dimensional homogeneous (in the plane of the layer) deformations of the director to which the treatments in Refs. 9, 24, and 25 were limited. Moreover, we cannot *a priori* ignore the real structure of a sample in which the liquid crystal is separated from the metal electrode by a layer of an orienting or some other substance (Fig. 2) in spite of the fact that the orienting layer can be, for example, hundreds of times thinner than the nematic layer. Since these layers are of submicron thickness and information about them is insufficient, their parameters are partly phenomenological. Bearing this point in mind, we shall adopt a thermodynamic description of a phase transition in the investigated system subjected to an external electric field.

We shall consider a liquid crystal layer of thickness D placed between electrodes which are subjected to an external static voltage U. The electrodes are coated with a layer of a suborienting substance of thickness $d \ll D$ (Fig. 7) which is characterized by isotropic distributions of the permittivity ε_s and an electrical conductivity σ_s. The z axis is perpendicular to the electrodes and their surfaces coincide with the $z = -d$ and $z = D + d$ planes (Fig. 7).

At a given value of U the equilibrium state of the whole system corresponds to a minimum of the functional $F = F_e + F_\varepsilon + F_f + F_\rho + F_W$, which is equal to the sum of the elastic F_e and flexoelectric F_f contributions of the nematic, of the dielectric contribution $F_\varepsilon = F_{\varepsilon N} + F_{\varepsilon S}$ of the nematic and of the orienting layer, and the contributions of the surface polarization F_ρ and the energy F_W representing the anchoring of the nematic to the surface of the orienting layer S_α ($\alpha = 0$ or D), which are given by

$$F_e = \frac{1}{2}\int dV\,[K_1(\nabla\mathbf{n})^2 + K_2(\mathbf{n}[\nabla\mathbf{n}])^2 + K_3[\mathbf{n}[\nabla\mathbf{n}]]^2],$$

$$F_\varepsilon = -\frac{1}{8\pi}\int dV\,\varepsilon_{ij}E_iE_j,$$

$$F_f = -\int dV(\mathbf{P}_f\mathbf{E}), \quad F_\rho = -\sum_{\alpha=+,0}\int dS_\alpha(\mathbf{P}_{s\alpha}\mathbf{E}), \tag{3}$$

$$F_W = \frac{1}{2}\sum_{\alpha=+,0}\int dS_\alpha W_\alpha \sin^2\theta|_{z=\alpha}.$$

Here, K_1, K_2, and K_3 are the Frank constants; ε_{ij} and E_j are the components of the permittivity tensor (of the NLC or the orienting layer) and of the electric field vector; W_α is the Rapini–Popular constant for the energy of anchoring of an NLC to the surface S_α; the repeated indices i and j imply summation. The electric field vector $\mathbf{E} = \mathbf{E}_0 - \nabla\varphi$, where $\mathbf{E}_0$ is the field directed along the z axis when the director orientation, is homeotropic:

$$E_{0i}(z) = \begin{cases} E_N = \pm\dfrac{U}{D'}, & 0 \leqslant z < D, \\ E_\alpha = \pm\dfrac{\sigma_\perp}{\sigma_\alpha}\dfrac{U}{D'}, & -d < z < 0, \quad D < z < D+d, \end{cases} \tag{4}$$

$$D' = D + 2d(\sigma_\perp/\sigma_\alpha).$$

The plus and minus signs in the system (4) correspond to the direction of the field $\mathbf{E}_0$ in the A and C cells, respectively (Fig. 7). We shall show later that it is sufficient to introduce one angle θ between the z axis and the vector $\mathbf{n}$ in order to parametrize the director. We can then say that $\mathbf{E}_0$ is the field for which we have $\theta = 0$, whereas $\nabla\varphi$ is the change in the field due to rotation of the director, i.e., it corresponds to $\theta \neq 0$; it follows from $U = \text{const}$ that the boundary condition on φ is:

$$\varphi_{z=-d} - \varphi_{z=D+d} = 0, \tag{5}$$

where $\varphi_{z'}$ denotes $\varphi(z = z')$.

In the cases of interest to us the tensor ε_{ij} for the nematic is of the second rank and has the following nonzero components:

$$\varepsilon_{xx} = \varepsilon_\parallel \sin^2\theta + \varepsilon_\perp\cos^2\theta, \quad \varepsilon_{zz} = \varepsilon_\parallel\cos^2\theta + \varepsilon_\perp\sin^2\theta,$$
$$\varepsilon_{xz} = \varepsilon_{zx} = \Delta\varepsilon\sin\theta\cos\theta,$$

where $\Delta\varepsilon = \varepsilon_\parallel - \varepsilon_\perp$; in the case of the orienting layer, we have $\varepsilon_{ij} = \varepsilon_S\delta_{ij}$. The tensor ε_{ij} corresponds to the stripe domain symmetry; for circular domains all that is necessary is the replacement of the index y in ε_{ij} simply with the index ρ. The conductivity tensor is obtained everywhere by replacing $\varepsilon_\parallel$, $\varepsilon_\perp$, ε_S, and $\Delta\varepsilon$ with $\sigma_\parallel$, $\sigma_\perp$, σ_S, and $\Delta\sigma$, respectively.

The potential φ is related to the director by the equation of continuity for the current vector $\mathbf{J}$ with the components $J_i = \sigma_{ij}E_j$:

$$\partial_i(\sigma_{ij}E_j) = 0, \tag{6}$$

where $\partial_i \equiv \partial/\partial x_i$. The components of the electric field at the interfaces S_α between the nematic and the orienting layers satisfy the following boundary conditions:

$$\sigma_\alpha E_z|_{z=\alpha-0} = (\sigma_{ij}E_j)|_{z=\alpha+0}, \quad \alpha = 0, \tag{7}$$

$$E_i(z=-0) = E_i(z=+0), \quad \alpha = 0, \tag{8}$$

$$(\sigma_{ij}E_j)|_{z=D-0} = \sigma_\alpha E_z|_{z=D+0}, \quad \alpha = D, \tag{9}$$

$$E_i(z=D-0) = E_i(z=D+0), \quad \alpha = D, \tag{10}$$

where E_i is the component of the electric field parallel to the plane of the layer. An important simplification of the calculations, which does not make any fundamental changes, results from neglect of the deformations of the director near one of the surfaces of the nematic (upper surface) compared with the deformations near the other (lower) surface: $\theta(z = D) \ll \theta(z = 0)$. The last inequality is fairly obvious if we make the above analysis of the deformations of the director in the electrooptic effect under consideration here.

Since φ can be expressed nonlocally in terms of θ using Eq. (6), F is a nonlocal functional of the function θ. Nevertheless, the problem of small deviations of the director (we recall that the angles found experimentally are within the range $\theta \lesssim 10°$) from the homeotropic state, when F is a quadratic function of θ and φ, can be solved by adopting the representation of θ and φ in the form of expansions of the complete system of functions with the appropriate symmetry. However, in the case of large variations of the material constants it is found that terms of the $\int(\nabla\varphi)^2 dV$ type in F are proportional to a very small quantity

$$\eta^2 = \left(\frac{\Delta\sigma d}{\sigma_\alpha D}\right)^2 \approx \left(\frac{1}{30}\right)^2$$

and can be included as corrections using perturbation theory. In the Appendices given below we shall consider separately the states which are homogeneous in the plane of the layer and/or periodic (Appendix I) as well as circular domains (Appendix II).

6. Hierarchy of domain structures in a nematic

A comparison of the values of f_0, f_y, and f_ρ described by Eqs. (I12), (I22), and (II2) in the Appendices, which are normalized to the functional F and are calculated, respectively, for the homogeneous (in the plane of the layer) state, and for stripe and circular domains, demonstrates that in the presence of the conductivity anisotropy $\Delta\sigma \neq 0$ and of an orienting layer $d \neq 0$ or of the surface polarization P_S, or both, the critical condition $f = 0$ for the transition $\theta_0 \neq 0$ is most difficult to satisfy for f_0. In the limit $d \to 0$ the main reason for this is the presence in terms $\sim\int\partial_i\varphi dy$ which do not vanish in the state homogeneous in the plane of the layer and which give rise to the second term associated with $|P_sE_N|$ in Eq. (I.12). If $P_s \to 0$, the reason for this behavior is an additional negative contribution $\sim -\varepsilon_S E_N^2(\Delta\sigma/\sigma_S)^2 d$ to f_y and f_ρ, which represents the dielectric energy of the orienting spacer. Naturally, the two factors can operate simultaneously. When they both disappear ($d = P_s = 0$), there are no differences beween f_0, f_y, and f_ρ. It should be pointed out that if $P_s \gtrsim 0$ and $d \gtrsim 0$, it follows from Eqs. (I22), (II2), and (I16) that if $q_1 = q_\parallel$, the state is inhomo-

geneous, but its period is large, since q_y and q_ρ are very small.

The expressions for f_y given by Eq. (II22) and for f_ρ given by Eq. (II2) lead to equality of the threshold conditions and, particularly, to $E_{1y} = E_{1\rho}$ for the same parameters of the layers (the additional factor in front of f_ρ naturally does not occur in the threshold condition). At the transition point we have $f_y = f_\rho = 0$, and the question which domain state is realized after the transition cannot be answered within the framework of the functional F which is quadratic in θ, and can only be solved if we introduce terms of the order of θ_0^3 and θ_0^4 in the expansion for this functional near the transition:

$$\Delta f_y = f_y\theta_0^2 + f_y^{(3)}\theta_0^3 + f_y^{(4)}\theta_0^4, \tag{11}$$

$$\Delta f_\rho = f_\rho\theta_0^2 + f_\rho^{(3)}\theta_0^3 + f_\rho^{(4)}\theta_0^4. \tag{12}$$

Fortunately, this problem can be solved without rigorous calculation of the coefficients $f^{(3)}$ and $f^{(4)}$ in Eqs. (11) and (12). We shall show that the phase transition from the homogeneous state to the stripe domains is a phase transition of the second order, whereas the transition to circular domains is of the first order. In fact, the coefficient is $f_y^{(3)} = 0$, since it consists of integrals of the type

$$\int_0^{L_y} dy \sin^3(q_y y),$$

which vanish identically. Therefore, it follows from the Landau theory that near the critical point $f_y = 0$ the amplitude obeys $\theta_{0y} \propto (-f_y)^{1/2}$ (on condition that $f_y^{(4)} > 0$, which is satisfied). On the other hand, integrals of the type

$$\int_0^R \rho\, d\rho\, J_1^2(q_\rho\rho)\, dJ_1(q_\rho\rho)/d\rho$$

do not vanish. For example, the third variation of the elastic Frank energy $f_{\rho F}^{(3)}\theta_0^3$ is proportional to the expression

$$f_{\rho F}^{(3)} \sim \frac{g}{(\max J_1)^3}(4K_{11}+K_{33}) \int_0^{R_0} J_1^3(x)\, dx,$$

which is the most important (in terms of magnitude) contribution to $f_\rho^{(3)}$, since $f_\rho^{(3)} > 0$. In this case the amplitude changes abruptly at the moment of the transition $f_\rho = 0$ and the change is

$$\theta_{0\rho} = \begin{cases} -\dfrac{3f_\rho^{(3)}}{4f_\rho^{(4)}}\left[1 - \dfrac{8f_\rho f_\rho^{(4)}}{9(f_\rho^{(3)})^2}\right], & f_\rho < 0 \\ 0, & f_\rho \geqslant 0 \end{cases} \tag{13}$$

Therefore, near the threshold when $|f_\rho|$ is sufficiently small, we always have the inequality

$$|\Delta f_\rho[\theta_{0\rho}(f_\rho)]| > |\Delta f_y[\theta_{0y}(f_y)]|,$$

because Δf_ρ changes abruptly, whereas Δf_y changes continuously. Therefore, a lattice of circular domains corresponds to a smaller value of the functional Δf and, consequently, this state is realized after the transition (naturally, if there is no preferred direction on the surface). On the other hand, after a jump the amplitude $\theta_{0\rho}$ rises much more slowly than θ_{0y}: $\theta_{0\rho} \propto (f_\rho + \text{const})$ [see Eq. (13)], which should be compared with $\theta_{0y} \propto (-f_y)^{1/2}$. Bearing in mind that Δf_ρ is still proportional to $g < 1$, we can expect that at sufficiently high values of $E - E_{c1}$ the potential barrier separating the states of the circular and stripe domains that have already appeared is very small. In this situation in the search for the states with a higher value of the geometric factor g the system may reach a "compromise" by pulling circular domains into an elongated shape. It is interesting to note that in our experiments some of the circular domain samples, in which there was no orienting layer and, consequently, the value of d was small [this was precisely the case when the values of $(-f_\rho)$ and $(-f_y)^{1/2}$ differed greatly in magnitude], became elongated and assumed a shape intermediate between circular and stripe domains.

The surface polarization $|P_s|$ can be found from the critical condition $f_\rho = 0$ or $f_y = 0$:

$$|P_s| = \frac{W_s - eE_N + K_3 q_\perp - (E_N^2/4\pi)(\Delta\sigma/\sigma_a)^2 \varepsilon_a d(\gamma q_\perp)^2}{|E_N|[1 + 2(\Delta\sigma/\sigma_a) d(q_\perp^2\gamma)]}, \tag{14}$$

where $E_N = \pm U_c/D'$, whereas $q_\perp$ denotes either q_y or q_ρ. In calculations based on Eq. (14) we can use the experimental values $d \approx 0.1\ \mu$m and the values of $q_\perp$, which are $2\pi/L_y$ for stripe domains and $\mu_1/R \approx 3.83/R$ for circular domains. We shall carry out calculations for stripe domains. Two independent methods[26] for determination of the anchoring energy give $W_{0C} = 5\times 10^{-3}$ dyn/cm and $W_{0A} = 2\times 10^{-3}$ dyn/cm. For a C cell of thickness $D = 80\ \mu$m we can expect domains with the period $L_y = 150\ \mu$m to appear at $U_c = 1.25$ V (Table I). A calculation carried out using Eq. (14) gives $P_{sC} = 10^{-2}$ dyn$^{1/2}$. In the case of an A cell if we assume that $D = 60\ \mu$m, $U_c = 0.7$ V, and $L_y = 115\ \mu$m, we find that $P_{sA} \approx 0.9\cdot 10^{-2}$ dyn$^{1/2}$.

This preference for a domain structure rather than for a homogeneous state, deduced from a comparison of the expressions for f_0 and f_y or f_ρ, means that the transition to a domain structure occurs earlier than to a homogeneous state. Knowing P_s we can now illustrate with specific numbers the fact that the transition to a homogeneous state, if possible, should occur at much lower values of the threshold voltage U_{0c} than the critical voltage U_c for the transition to the domain structure. In fact, we can find U_{0c} by equating Eq. (I14) to zero and using in it the values of P_s just found:

$$U_{0c} = \left(W_s - \frac{\Delta\sigma}{\sigma_a t_a D'}\right)\left[P_s\left(1 - 2\frac{\Delta\sigma}{\sigma_a}\right) \pm e - K_3 t_a\right]^{-1},$$

where the plus corresponds to an A cell and the minus to a C cell. A calculation using $P_{sC} = 10^{-2}$ dyn$^{1/2}$ and $P_{sA} = 0.9\times 10^{-2}$ dyn$^{1/2}$ gives $U_{0C} \approx 1.6$ V and $U_{0A} \approx 0.9$ V. Comparing these results with the experimental values for the transition to a domain structure, $U_{cC} \approx 1.25$ V and $U_{cA} \approx 0.7$ V, we can see that $U_c < U_{0c}$. In the final analysis this is the reason for the appearance of a domain structure when $U = U_c$.

CONCLUSIONS

We thus demonstrated experimentally and theoretically that the surface polarization of a nematic crystal may be manifested in the electrooptic effects. The estimated value of the polarization ($\lesssim 10^{-2}$ dyn$^{1/2}$) is sufficiently high for the

director instability induced by this polarization to be manifested even in the presence of a stabilizing influence of other mechanisms, particularly of the dielectric and flexoelectric effects. It is important to note that the experimentally observed three-dimensional structure of deformations can be explained theoretically in a natural manner. Therefore, in the absence of the surface polarization a structure of this kind does not appear and the domains themselves can be used as the criterion of its appearance.

Domain structures have been observed recently in those cases when the equilibrium deformation of a nematic has been assumed to be *a priori* homogeneous in the plane of the layer, for example, in the case of the Fréedericksz transition[27] or in a hybrid cell.[28] The present paper adds one more effect to this list.

The authors are grateful to Kh. Khinov for valuable discussions and to A. V. Koval'chuk for his help in the experiments.

APPENDIX I. DEFORMATIONS OF THE DIRECTOR IN A PLANE SET BY THE PREFERRED DIRECTION ON A SURFACE IN CONTACT WITH A NEMATIC

Rubbing of the orienting surface aligns the director in the yz plane (Fig. 7), $\mathbf{n} = (0, \sin\theta, \cos\theta)$, $\theta = \theta(y, z)$, and the twist deformation is impossible. If we consider only small values of θ and φ, we can find the functional F accurate to within the terms which are quadratic in these functions:

$$F_v = \frac{1}{2}\int dy \int_0^D dz\,[K_1(\partial_y\theta)^2 + K_3(\partial_z\theta)^2]. \tag{I1}$$

$$F_s = F_{sE} + F_{sK},$$

$$F_{sE} = -\frac{\varepsilon_a}{8\pi}\int dy \left(\int_{-d}^{0} + \int_{D}^{D+d}\right) dz\,[(\nabla\varphi)^2 - 2E_x\partial_z\varphi], \tag{I2}$$

$$F_{sK} = -\frac{1}{8\pi}\int dy \int_0^D dz\,[-\Delta\varepsilon E_K\theta^2 - 2\varepsilon_a E_K\partial_z\varphi + \varepsilon_\parallel(\partial_z\varphi)^2 + \varepsilon_\perp(\partial_y\varphi)^2 - 2\Delta\varepsilon E_K\theta\,\partial_y\varphi], \tag{I3}$$

$$F_l = \int dy \int_0^{D'} dz\,(eE_K\theta\,\partial_z\theta + e_1\partial_z\varphi\,\partial_y\theta + e_3\partial_y\varphi\,\partial_z\theta - e_1E_K\partial_y\theta), \tag{I4}$$

$$F_p = \int dy \left(\frac{1}{2}E_K P_z\theta^2 + P_z\theta\partial_y\varphi + P_z\partial_z\varphi\right)\Big|_{z=+0}, \tag{I5}$$

$$F_w = -\frac{1}{2}\int dy\, W_z\theta^2|_{z=0}. \tag{I6}$$

The last term in Eq. (I4) is linear in θ, but it differs from zero only if there is an abrupt change in the angle θ at a domain boundary. The value of each functional F is assumed to be the value per unit length along a domain (along the x axis).

A. Nematic with a state homogeneous in the layer plane

In the case when the distribution is homogeneous along y ($\partial_y = 0$), the Euler–Lagrange equations for the functional (I2) describing φ in an orienting layer are identical with the equation of continuity of the current given by (6):

$$\frac{d}{dz}\partial_z\varphi = 0, \quad -d < z < 0, \quad D < z < D+d. \tag{I7}$$

However, in the case of a nematic, Eq. (6) becomes more complex:

$$\frac{d}{dz}(\sigma_1\partial_z\varphi + \Delta\sigma E_K\theta^2) = 0, \quad 0 < z < D. \tag{I8}$$

These equations are sufficient to see that in the case of a nematic the value of φ is a quadratic functional of θ:

$$\varphi(z) \sim \int_0^z \theta^2\,dz + \text{const}\cdot z.$$

After substitution in Eqs. (I1)–(I6), the solutions of Eqs. (I7) and (I8) subject to the boundary conditions (5), (6), and (9) yield the following expression for the part of the functional F which is quadratic in φ and which we can denote here by F_0:

$$\frac{F_0}{L_y} = \int_0^D dz \left\{\frac{K_3}{2}(\partial_z\theta)^2 + \frac{E_K}{8\pi}\left[\Delta\varepsilon + 4\left(\varepsilon_a\frac{\sigma_1}{\sigma_a} - \varepsilon_1\right)\frac{\Delta\sigma d}{\sigma_a D'}\right]\theta^2\right\} + \frac{1}{2}(E_K P_z - eE_K + W_0)\theta_0^2 + P_z(\partial_z\varphi)|_{z=+0}, \tag{I9}$$

where L_y represents the dimensions of the system. The Euler–Lagrange equation for the functional of Eq. (I9) is readily solved and the solution is

$$\theta = \theta_0\exp(-q_0 z), \quad q_0 = E_K t_0,$$

$$t_0 = \left\{\frac{1}{4\pi K_3}\left[\Delta\varepsilon + 4\left(\varepsilon_a\frac{\sigma_1}{\sigma_a} - \varepsilon_1\right)\frac{\Delta\sigma d}{\sigma_a D'}\right]\right\}^{-1/2}. \tag{I10}$$

We shall give also the expression for the change in the field $-\partial_z\varphi$, due to a tilt of the director by an angle $\theta(z)$:

$$-\partial_z\varphi = \begin{cases} \dfrac{\Delta\sigma}{\sigma_1}E_K\theta_0^2\left[\exp(-2q_0 z) - \dfrac{1}{2q_0 D'}\right], & 0 < z < D \\ -\dfrac{\Delta\sigma}{\sigma_a}\dfrac{E_K}{2q_0 D'}\theta_0^2, & -d < z < 0, \quad D < z < D+d \end{cases}. \tag{I11}$$

We can see that the orienting layer of Eq. (I11) contains a factor $\Delta\sigma/\sigma_S \approx 14$, because of which the dielectric contribution of this layer can be significant in spite of its small thickness. Equation (I10) demonstrates this clearly: the second term in the square brackets is proportional to a small quantity $10^{-4} < d/D' < 10^{-2}$, but on the whole it is of the same order of magnitude as the first term $\Delta\varepsilon$.

The final expression for the functional F_0 is obtained by substituting Eqs. (I10) and (I11) into Eq. (I9):

$$f_0 = \frac{F_0}{L_y\theta_0^2} = \frac{1}{2}(K_3 q_0 + W_0 - E_K e) - |P_z E_K| \times\left[\frac{1}{2} - \frac{\Delta\sigma}{\sigma_1}\left(1 - \frac{1}{2q_0 D'}\right)\right], \tag{I12}$$

where it is assumed that the vector $\mathbf{P}_z$ (at the anode in an A cell and at the cathode in the C cell) is antiparallel to the vector $\mathbf{E}_K$.

B. Stripe domains in a nematic

We shall now consider a domain structure periodic in y. Since the functionals (I1)–(I6) and Eqs. (6)–(10) modified to allow for the expressions described in $\varepsilon_{ij}(\theta)$ and $\sigma_{ij}(\theta)$ are invariant under the transformation $y \to -y$,

$\theta \to -\theta$, the functions $\theta(y) = -\theta(y)$ can be represented as a Fourier sine series:

$$\theta(z, y) = \theta_0 \sum_{n=1}^{\infty} \psi_n(z) \sin(nq_y y),$$

where $q_y = 2\pi/L_y$ is the wave number of the domain structure and $\theta_0 \ll 1$. As in the homogeneous case, we can express the potential φ in terms of θ, by writing down the equation of continuity of the current (6). In this case this equation for a nematic contains terms linear in θ:

$$\sigma_\perp \partial_z^2 \varphi + \sigma_\parallel \partial_z^2 \varphi = \Delta\sigma E_N \partial_y \theta. \tag{I13}$$

The Euler–Lagrange equation of the functional (I2) for φ in the orienting layer is still identical with the equation of continuity (6):

$$\partial_z^2 \varphi + \partial_y^2 \varphi = 0. \tag{I14}$$

It follows from Eqs. (I13) and (I14), and from the form of $\theta(z, y)$ that, firstly, φ has the form of the Fourier series in terms of the cosines

$$\varphi(y, z) = \sum_{n=1}^{\infty} \varphi_n(z) \cos(nq_y y),$$

and, secondly, φ_n and together with them the whole function φ constitute effectively a functional which is linear in θ. This is sufficient to select, from the functionals (I1)–(I6), the necessary part which is quadratic in θ. As pointed out in Sec. 5, in the case of a domain structure in a nematic, we have $\varphi_N \propto \eta$, where $\eta \ll 1$, so that the terms containing φ_N can be omitted in the first approximation. On the other hand, the z component of the field $\partial_z \varphi_S$ in the orienting layer is considerably greater than in the nematic, so that its dielectric contribution F_{zS} of Eq. (1.2) should be allowed for. Substituting the series $\theta(y, z)$ and $\varphi(y, z)$ into Eqs. (I1)–(I6) and then integrating with respect to the variable y within one period L_y, we obtain a functional F which in the case of stripe domains will be denoted by F_y:

$$\begin{aligned}\frac{2F_y}{L_y} = \theta_0^2 \sum_{n=1}^{\infty} \Bigg\{ \int_0^D dz \Big[&\frac{1}{2} K_3 (\partial_z \psi_n)^2 \\ &+ \Big(\frac{1}{2} K_1 q_y^2 n^2 + \frac{\Delta\varepsilon E_N^2}{8\pi} \Big) \psi_n^2 \Big] \\ &- \frac{\varepsilon_S}{8\pi} \Big(\int_{-d}^{0} + \int_{D}^{D+d} \Big) dz \left[(\partial_z \varphi_n)^2 + q_y^2 n^2 \varphi_n^2 \right] \\ &+ \frac{1}{2} (E_N P_s + W_0 - eE_N) \psi_n^2 |_{z=0} \\ &+ P_s q_y n (\psi_n \varphi_n)|_{z=0} \Bigg\}. \end{aligned} \tag{I15}$$

The Euler–Lagrange equation for the functional (I15) describing ψ_n in a nematic layer is readily solved:

$$\begin{gathered}\psi_n = \psi_{0n} \exp(-q_n z), \quad q_n^2 = \frac{K_1}{K_3} q_y^2 n^2 + t^2 E_N^2, \\ t = \left(\frac{\Delta\varepsilon}{4\pi} \right)^{1/2}, \end{gathered} \tag{I16}$$

where ψ_{0n} are constants. Knowing explicitly the form of $\psi_n(z)$, we can write down Eqs. (I13) and (I14) for the harmonics of the potential $\varphi_n(z)$:

$$\sigma_\parallel \partial_z^2 \varphi_n - \sigma_\perp q_y^2 n^2 \varphi_n = \Delta\sigma E_N q_y n \theta_0 \psi_{0n} \exp(-q_n z), \quad 0 < z < D, \tag{I17}$$

$$\partial_z^2 \varphi_n - n^2 q_y^2 \varphi_n = 0, \quad -d < z < 0, \quad D < z < D+d. \tag{I18}$$

The solution of Eq. (I17) is the sum of its general solution without the right-hand part (containing for each harmonic two constants a_n and b_n) and the particular solution, which is found to be:

$$\begin{aligned}\varphi_n(z) = \frac{\Delta\sigma}{\sigma_\parallel} \frac{E_N \theta_0 q_y n}{q_n^2 - \beta q_y^2 n^2} \{ &a_n \exp(-\beta^{1/2} q_y n z) \\ &+ b_n \exp(\beta^{1/2} q_y n z) + \exp(-q_n z) \}, \\ \beta = \sigma_\perp / \sigma_\parallel, \quad &0 < z < D. \end{aligned} \tag{I19}$$

We shall not give the solution of Eq. (I18) or the expressions for the constants a and b because they are too cumbersome. We shall only give the expressions for $\varphi_n(z = +0)$ and $\partial_z \varphi_n$ in the orienting layer, which occur in Eq. (I15):

$$\varphi_n(z = +0) = -\frac{\Delta\sigma}{\sigma_\parallel} d q_y n \gamma_n \theta_0 \psi_{0n} E_N,$$

$$\partial_z \varphi_n(z) = \begin{cases} \dfrac{\Delta\sigma}{\sigma_\parallel} q_y n \gamma_n \theta_0 \psi_{0n} E_N, & -d < z < 0 \\ 0, & D < z < D+d, \end{cases} \tag{I20}$$

$$\gamma_n^{-1} = (1 + nq_y d \beta^{1/2} \sigma_\perp / \sigma_\parallel)(q_n + \beta^{1/2} n q_y). \tag{I21}$$

Substituting these expressions into Eq. (I15), we obtain the functional in the form of a sum of the contributions of all the harmonics. However, it is shown in Appendix III that at the moment of a phase transition, which accompanies the electrooptic effect under consideration, only the first harmonic appears in a domain structure. Therefore, we shall give only its contribution to F_y on the assumption that $\psi_{01} = 1$ and $\psi_{0n} = 0$ where $n > 1$, $q_1 = q_\parallel$, $\gamma_1 = \gamma$, where q_1 and γ_1 are determined in Eqs. (I16) and (I21):

$$\begin{aligned} f_y = \frac{2F_y}{L_y \theta_0^2} = \frac{1}{2}(K_1 q_y^2 + W_0 - eE_N) - |P_s E_N| \left(\frac{1}{2} + \frac{\Delta\sigma}{\sigma_\parallel} q_y^2 d\gamma \right) \\ - \frac{\varepsilon_S E_N^2}{8\pi} (q_y \gamma)^2 \left(\frac{\Delta\sigma}{\sigma_\parallel} \right)^2 d. \end{aligned} \tag{I22}$$

The expression (I22) still contains an undetermined parameter q_y, which is the wave number of the domain structure. We can find it by minimizing Eq. (I22) with respect to q_y, i.e., by solving equation $\partial F_y / \partial q_y = 0$, but subject to the conditions that $q_\parallel = q_\parallel(q_y)$ and $\gamma = \gamma(q_y)$. In principle, we can use this equation to find the wave number and the functions U and P_s [U and E_N are related by Eq. (4)] and other parameters of the problem, which for the sake of brevity we did not include in the arguments of the function q_y. After this, substituting $q_y(U, P_s)$ into Eq. (I22), we obtain the value of the function F for given values of the external and internal parameters. Equating this expression to zero, i.e., solving the equation

$$F_y(U_c, P_s, q_y(U_c, P_s)) = 0$$

we can find either the critical voltage $U_c(P_s)$ or the surface polarization $P_s(U_c)$ from the critical voltage. However, it is not possible to solve analytically the equation $\partial F_y / \partial q_y = 0$, which was the reason why in Sec. 6 we found P_s from the equation $F_y(U_c, P_s, q_y) = 0$ using the experimental values of $q_y = 2\pi/L_y$ (Fig. 3b) and of U_c.

The expression (I22) does not reduce to Eq. (I12) for F_0 if $q_y = 0$, since in the field case the terms $\int_{L_y} \partial_x \varphi dy$ in Eqs. (I2), (I3), and (I5) do not contribute to F_y even when $q_y \to 0$, whereas in the homogeneous case these integrals are finite. This is the reason why we considered separately the domain structure and the homogeneous state.

APPENDIX II. LATTICE OF CIRCULAR DOMAINS IN A NEMATIC

If a specific orientation of the director is not specified on the interfaces with the nematic, the distribution of the director ceases to be planar and an electrooptic transition creates a circular domain structure (Fig. 3a). Figure 8 shows a distribution of the domains corresponding to the closest packing or the largest value of the factor g, which is equal to the ratio of the domain area to the total area of the nematic layer. This ratio can be found by considering the triangle shown in Fig. 8, and its value is $g = \pi/2\times 3^{1/2} \approx 0.91$.

We shall consider one of the components of the structure of circular domains. Let us assume that the z axis passes through the center of the structure, that ρ is the distance from the z axis, and that there is no dependence on the azimuthal angle Φ: $\partial/\partial\Phi = 0$. We can easily show that under these assumptions the terms containing Φ and n_Φ in the expression for the elastic energy of the nematic, including those corresponding to the twist deformation, are of the third order in θ and Φ, so that it is again sufficient to consider just the angle θ when parametrizing the director.

By analogy with the case of stripe domains we can show that φ is a linear functional with respect to θ and that in the expression for a circular domain the terms of the type

$$\int_0^R \rho\, d\rho\, \partial_x \varphi$$

vanish. Therefore, the quadratic part of the function F for N_D domains, which in this case will be denoted by F_ρ, is of the form

$$F_\rho = N_D 2\pi \int_0^R \rho\, d\rho \left\{ \int_0^D dz \left[-\frac{K_1}{2}\theta L_\rho \theta + \frac{K_3}{2}(\partial_z\theta)^2 + \frac{\Delta\varepsilon E_N^2}{8\pi}\theta^2 \right] - \frac{\varepsilon_a}{8\pi}\left(\int_{-d}^{0} + \int_{D}^{D+d} \right) dz (\nabla\varphi)^2 + \frac{1}{2}(E_x P_x + W_0 - eE_N)\theta^2|_{z=0} + P_x(\theta\partial_\rho\varphi)|_{z=0} \right\}. \quad \text{(II1)}$$

where

$$L_\rho = \frac{\partial^2}{\partial\rho^2} + \frac{\partial}{\rho\partial\rho} - \frac{1}{\rho^2}.$$

The eigenfunctions $Y_n(\rho)$ of this operator, satisfying the conditions $Y_n(R) = Y_n(0) = 0$ on the domain boundaries, are the first-order Bessel functions $J_1(\mu_n\rho/R)$, where μ_n is the nth root of the function $J_1(x)$. Therefore, by analogy with the solution for stripe domains, the problem of circular domains can be solved in the form of expansions:

$$\theta(\rho, z) = \sum_{n=1}^{\infty} Z_n(z) J_1(\mu_n\rho/R), \quad \varphi(\rho, z) = \sum_{n=1}^{\infty} \varphi_n(z) J_0(\mu_n\rho/R),$$

and at the moment of the transition once again only one harmonic appears and its radial wave number is $q_\rho = \mu_1/R$,

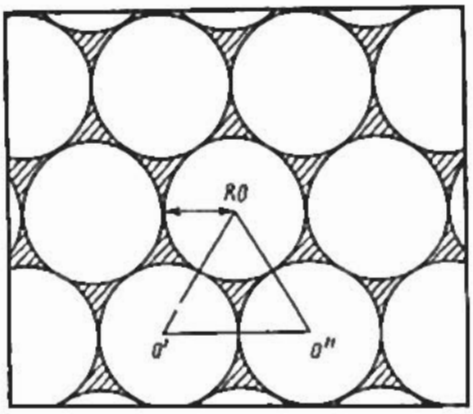

FIG. 8. Packing of circular domains in the plane of a nematic layer. Homeotropic orientation of the director is retained in the gaps between the domains (shown shaded).

where $\mu_1 \approx 3.83$. If N_D is sufficiently large, then F_ρ normalized to the total area of the layer S is described by

$$f_0 = \frac{2F_\rho}{S\theta_0^2} = g\left(\frac{J_2(\mu_1)}{\max J_1}\right)^2 \left\{ \frac{1}{2}(K_3 q_\parallel^2 + W_0 - eE_N) - |P_x E_N| \left[\frac{1}{2} + \left(\frac{\Delta\sigma}{\sigma_a}\right)^2 q_\rho^2 d\gamma \right] - \frac{\varepsilon_a E_N^2}{8\pi}(q_\rho\gamma)^2 \left(\frac{\Delta\sigma}{\sigma_a}\right)^2 d \right\}. \quad \text{(II2)}$$

The factor $J_2(\mu_1)/\max J_1$ is introduced to ensure that the value of θ_0 is the amplitude of the first harmonic; $q_\parallel$ and γ are found, respectively, from Eqs. (I16) and (I21) if q_y is replaced with q_ρ when $n = 1$.

APPENDIX III

The final expression for the functional F_y of Eq. (I15) is the sum of the contributions of an infinite series of harmonics:

$$2F_y/L_y = \theta_0^2 \sum_{n=1}^{\infty} F_n \psi_{0n}^2,$$

$$F_n = \frac{1}{2}(K_3 q_n^2 + W_0 - eE_N) - |P_x E_N| \left(\frac{1}{2} + \frac{\Delta\sigma}{\sigma_a} q_y^2 n^2 d\gamma_n^2 \right) - \frac{\varepsilon_a E_N^2}{8\pi}(q_y n\gamma_n)^2 \left(\frac{\Delta\sigma}{\sigma_a}\right)^2 d. \quad \text{(III1)}$$

The condition for the appearance of the electrooptic domain effect is the excitation of at least one harmonic. The critical condition for the appearance of the nth harmonic is

$$\min_{q_y} F_n = 0,$$

since q_y is still the free parameter. We note that F_n depends only on the combination $q_y n$, $F_n(q_y) = F_1(q_y n)$, so that we have

$$\frac{\partial}{\partial q_y} \sum_{n=1}^{\infty} F_n \psi_{0n}^2 = \sum_{n=1}^{\infty} \frac{\partial F_n}{\partial (q_y n)} n\psi_{0n}^2$$

and the condition for an extremum is q_y is

$$\partial F_1(z)/\partial z|_{z=q_y n} = 0.$$

Solving the above equation, we can express $q_y n$ as a function of E_N and P_x (and also for other parameters of the problem): $q_y n = Q(E_N, P_x)$. Since the right-hand side of this expression is independent of n, it follows that if $Q \neq 0$ (which is true

of all our experiments), then the condition $\partial F_n/\partial(q_y n) = 0$ can be satisfied for just one harmonic n_0 (otherwise we would arrive at the contradiction that $q_y = Q/n_0 = Q/n_0'$ when $n_0 \neq n_0'$) and, because $F_{n0}(Q/n_0) = F_1(Q)$, the value of n_0 can be always selected to be unity, which corresponds to $q_y = Q(E_N, P_s)$. Therefore, at the moment of a transition we can expect one (first) harmonic in the sum of Eq. (III1). This is true until the parameters of the problem change sufficiently for $F_2(Q)$ to vanish, when the second harmonic of the perturbation appears, etc. The amplitudes of these harmonics can be found only if we allow for the terms of the fourth order in θ. We shall not consider this point here, but confine ourselves only to the critical condition for the appearance of the first harmonic of the domain structure. However, it should be pointed out that in our experiments the appearance of the second harmonic corresponds to a reduction in the width of a stripe with the maximum brightness (and with a maximum angle θ) when the total number of the stripe domains observed sufficiently high above the field E_{c1} is constant.

[11] Some of the results in this section were published by us in a brief communication.[18]

[1] L. M. Blinov, *Electrooptics and Magnetooptics of Liquid Crystals* [in Russian], Nauka, Moscow (1987), p. 384.
[2] R. B. Meyer and P. S. Pershan, Solid State Commun. 13, 989 (1973).
[3] A. N. Chuvyrov, A. S. Sonin, and A. D. Zakirova, Fiz. Tverd. Tela (Leningrad) 18, 3084 (1976) [Sov. Phys. Solid State 18, 1797 (1976)].
[4] L. M. Blinov, E. I. Kats, and A. A. Sonin, Usp. Fiz. Nauk 152, 449 (1987) [Sov. Phys. Usp. 30, 604 (1987)].
[5] O. A. Skaldin and A. N. Chuvyrov, Fiz. Tverd. Tela (Leningrad) 28, 518 (1986) [Sov. Phys. Solid State 28, 289 (1986)].
[6] O. A. Skaldin, A. N. Lachinov, and A. N. Chuvyrov, Fiz. Tverd. Tela (Leningrad) 27, 1220 (1985) [Sov. Phys. Solid State 27, 734 (1985)].
[7] A. N. Lachinov and A. N. Chuvyrov, Poverkhnost' No. 5, 74 (1986).
[8] P. Guyot-Sionnest, H. Hsiung, and Y. R. Shen, Phys. Rev. Lett. 57, 2963 (1986).
[9] M. Monkade, Ph. Martinot-Lagarde, and G. Durand, Europhys. Lett. 2, 299 (1986).
[10] M. Nakagawa and T. Akahane, J. Phys. Soc. Jpn. 52, 3773 (1983).
[11] D. K. Rout and R. N. P. Choudhary, J. Phys. D 22, 289 (1989).
[12] M. Nakagawa and T. Akahane, J. Phys. Soc. Jpn. 52, 3782 (1983).
[13] A. G. Petrov and A. Derzhanski, Mol. Cryst. Liq. Cryst. Lett. 41, 41 (1977).
[14] H. Schad and M. A. Osmah, J. Chem. Phys. 75, 880 (1981).
[15] I. Dozov, Ph. Martinot-Lagarde, and G. Durand, J. Phys. Lett. 44, L817 (1983).
[16] E. M. Terent'ev and O. D. Lavrentovich, Zh. Eksp. Teor. Fiz. 91, 2084 (1986) [Sov. Phys. JETP 64, 1237 (1986)].
[17] E. J. Sinclair and E. F. Carr, Mol. Cryst. Liq. Cryst. 37, 303 (1976).
[18] O. D. Lavrentovich, V. M. Pergamenshchik, and V. V. Sergan, Zh. Tekh. Fiz. 60(1), 208 (1990) [Sov. Phys. Tech. Phys. 35, 127 (1990)].
[19] L. A. Beresnev, L. M. Blinov, S. A. Davidyan *et al.*, Pis'ma Zh. Eksp. Teor. Fiz. 45, 592 (1987) [JETP Lett. 45, 755 (1987)].
[20] M. J. Bradshaw, E. P. Raynes, J. D. Bunnig, and T. E. Faber, J. Phys. (Paris) 46, 1513 (1985).
[21] G. Barbero, I. Dozov, J. F. Palierne, and G. Durand, Phys. Rev. Lett. 56, 2056 (1986).
[22] I. Janossy, Europhys. Lett. 5, 431 (1988).
[23] I. Dozov, G. Barbero, J. F. Palierne, and G. Durand, Europhys. Lett. 1, 563 (1986).
[24] A. Derzhanski, A. G. Petrov, and M. D. Mitov, J. Phys. (Paris) 39, 273 (1978).
[25] G. Barbero and G. Durand, Phys. Rev. A 35, 1294 (1987).
[26] O. D. Lavrentovich, T. Ya. Marusii, Yu. A. Reznikov, and V. V. Sergan, Zh. Tekh. Fiz. 59(10), 199 (1989) [Sov. Phys. Tech. Phys. 34, 1219 (1989)].
[27] E. Lonberg and R. B. Meyer, Phys. Rev. Lett. 55, 718 (1985).
[28] O. D. Lavrentovich and V. M. Pergamenshchik, Pis'ma Zh. Tekh. Fiz. 15(5), 73 (1989) [Sov. Tech. Phys. Lett. 15, 194 (1989)]; Mol. Cryst. Liq. Cryst. 179, 125 (1990).

Translated by A. Tybulewicz